

# Isolation by Distance in the Spore-Forming Soil Bacterium *Myxococcus xanthus*

Michiel Vos<sup>1,3,\*</sup> and Gregory J. Velicer<sup>1,2</sup>

<sup>1</sup>Max-Planck Institute for Developmental Biology  
Tübingen 72076  
Germany

<sup>2</sup>Department of Biology  
Indiana University  
Bloomington, Indiana 47405

## Summary

Genetic differentiation between spatially separated populations within a species is commonly observed in plants and animals, but its existence in microbes has long been a contentious issue [1–5]. Traditionally, many microbial ecologists have reasoned that microbes are not limited by dispersal as a result of their immense numbers and microscopic size [2, 6]. In this view, the absence of barriers to gene flow between populations would prevent differentiation of populations by genetic drift and hinder local adaptation. *Myxococcus xanthus* is a globally distributed, spore-forming bacterium that offers a robust test for genetic differentiation among populations because sporulation is expected to enhance dispersal. Using multi-locus sequence data, we show here that both diversity and the degree of differentiation between populations increase as a function of distance in *M. xanthus*. Populations are consistently differentiated at scales exceeding 10<sup>2</sup>–10<sup>3</sup> km, and isolation by distance, the divergence of populations by genetic drift due to limited dispersal, is responsible. Our results provide new insights into how genetic diversity within species of free-living microbes is distributed from centimeter to global scales.

## Results and Discussion

Recent studies on extremophilic prokaryotes living in geothermal springs have challenged the idea that microbial populations are not limited by dispersal [3, 7, 8]. For example, geographic distance and genetic divergence, but not environmental differences, were found to correlate in the hyperthermophilic archaeon *Sulfolobus*, suggesting that genetic drift due to limited gene flow caused distant populations to diverge [8]. In another study, the presence of deleterious IS elements in isolated populations of *Pyrococcus* provided more direct evidence that genetic drift can cause divergence between extremophile populations [7].

Extremophiles are probably the most likely free-living microbes to exhibit isolation by distance; they inhabit small, isolated habitats, do not form spores, and require very specific conditions to survive. Successful dispersal events between distant extremophile populations are thus expected to be rare. However, many free-living microbes inhabit large and contiguous terrestrial or aquatic environments without

obvious barriers to gene flow. The handful of spatially explicit studies that have investigated the population structure of terrestrial prokaryotes indicate some degree of endemism due to local adaptation, isolation by distance, or both (e.g., [9–16]) but were relatively limited in their genetic and/or spatial resolution.

In this study, we investigated the population structure of the Gram-negative bacterium *Myxococcus xanthus*, which is found around the globe in a wide variety of soil habitats [17] and is not associated with a host. Upon starvation, this species forms conspicuous multicellular fruiting bodies that facilitate species identification and clone isolation [18]. The combination of its cosmopolitan distribution and its ability to form stress-resistant spores makes *M. xanthus* a conservative test case for the existence of population structure in a free-living microbe.

We tested for the presence of population structure against the null hypothesis that the genetic diversity in *M. xanthus* is homogeneously distributed across the globe as a result of ubiquitous dispersal and lack of differential local adaptation. Such absence of structure would be demonstrated by similar degrees of nucleotide diversity across all spatial scales. In contrast, when geographic isolation and/or local adaptation cause populations to diverge, larger spatial scales will house a larger number of distinct populations and greater nucleotide diversity. We first tested for population structure by comparing nucleotide diversity of *M. xanthus* clones isolated at incremental sampling scales.

A total of 145 *M. xanthus* clones were isolated from soil samples collected in a nested-sampling design spanning nine orders of magnitude. Each isolate was assigned to a sample set representing a distinct spatial scale (Table 1 and Table S1 in the Supplemental Data available online). As a measure of diversity, we surveyed the number and abundance of nucleotide polymorphisms in a concatemer of five conserved loci: *clpX*, *csgA*, *fibA*, *icd*, and *sglK*. Prokaryote diversity is usually estimated at the level of genotypes or alleles, but much higher resolution can be obtained with single-nucleotide polymorphisms.

We found that average nucleotide diversity ( $\pi$ ) increased significantly as a function of distance across the nested-isolate sets (Figure S1). However, because sample size differed across the sets, we controlled for this variation by performing a rarefaction analysis based on nucleotide richness; in this analysis, populations are repeatedly sampled at all possible sub-sample sizes so that the average richness at each size can be calculated. This approach allows (1) comparison of different sample sets via equal sampling efforts and (2) assessment of the degree to which sampled diversity represents actual diversity.

Figure 1 shows the rarefaction curves for the different sample sets. The number of isolates sub-sampled is shown on the x axis, and the total number of polymorphisms found is shown on the y axis. Sample sets D, E, and F (10<sup>1</sup>–10<sup>3</sup> m scales, Table 1) were combined for this analysis because of their relatively small size, which hindered comparison of curve trajectories. The rarefaction curve of the centimeter-scale population (set A) is lowest and levels off substantially, illustrating that most of the diversity present at that scale was sampled (Figure 1).

\*Correspondence: michiel.vos@zoo.ox.ac.uk

<sup>3</sup>Present address: Department of Zoology, University of Oxford, Oxford OX1 3PS, United Kingdom.

Table 1. Summary of Nested-Isolate Sets

Set	Location	n Clones	n Genotypes <sup>a</sup>	Average Distance between Isolates (Standard Deviation)
A	Tübingen	20	11	0.07 (0.03) m
B	Tübingen	26	16	0.54 (0.32) m
C	Tübingen	16	13	3.64 (1.79) m
D	Tübingen	8	7	47 (23) m
E	Tübingen	9	8	376 (228) m
F	Tübingen	6	4	878 (480) m
D-F combined	Tübingen	23	19	393 (N.A.) m
G	SW Germany	18	16	106 (640) km
H	Europe	23	22	1213 (608) km
I	World	19	19	9228 (4445) km

<sup>a</sup> Each genotype has a unique five-locus concatemer sequence (2331 bp).

Rarefaction curves are considered to be significantly different from each other if the observed diversity of one curve lies beyond the near 95% confidence interval of another curve [19]. The decimeter- and meter-scale populations (sets B and C, respectively) show successive and significant increases in diversity.

Interestingly, however, the diversity levels of the meter (set C),  $10^1$ – $10^3$  m (sets D–F) and regional (southwest Germany, set G) sample sets do not differ significantly from each other despite the fact that the sampling scales of these sets span more than four orders of magnitude. This indicates that a population at the meter scale can house a level of diversity approaching that contained in a large region hundreds of kilometers broad (Figure 1). The diversity plateau ends at larger scales; nucleotide richness rises greatly from the southwest German (set G) to the European (set H) and global (set I) scales.

We also compared estimates of total richness for each spatial scale by using the Chao1 richness estimator (Figure 2). This estimator relies only on observed data and ignores any rare polymorphisms not present in our samples; it therefore still underestimates actual total richness [20]. Although the observed diversities of sets C and D–F were not found to differ (Figure 1), the estimated total diversities of these sets do differ significantly (Figure 2). Sets D–F and G were not found to differ in either observed or estimated total diversity, whereas all other stepwise comparisons show significant increases in estimated total diversity with distance. Because the Chao1 estimator is itself dependent on sample size, we plotted Chao1 as a function of the number of sequences sampled and found that only the richness estimate for the global set would have been substantially higher had the sample size for each set been much larger (Figure S2).

Long-distance dispersal events are suggested by the occurrence of identical or near-identical concatemer genotypes at distant locations (Figure S3). Significant migration is to be expected in spore-forming bacteria and has been demonstrated previously [21]. However, identical genotypes were found primarily within the smaller spatial scales (sets A–F in Tübingen and set G in southwest Germany) in the nested-isolate set. Three of the Tübingen genotypes were found elsewhere in Germany, and one each was found in Switzerland, Italy, Croatia, and Sweden (Table S2).

At most locales from which isolates for sets G, H, and I were obtained, ten soil samples were collected at 1 m intervals in a linear transect. Only the first isolate per transect was used in the nested-isolate set described above. However, when six or more isolates were obtained from a single transect, they

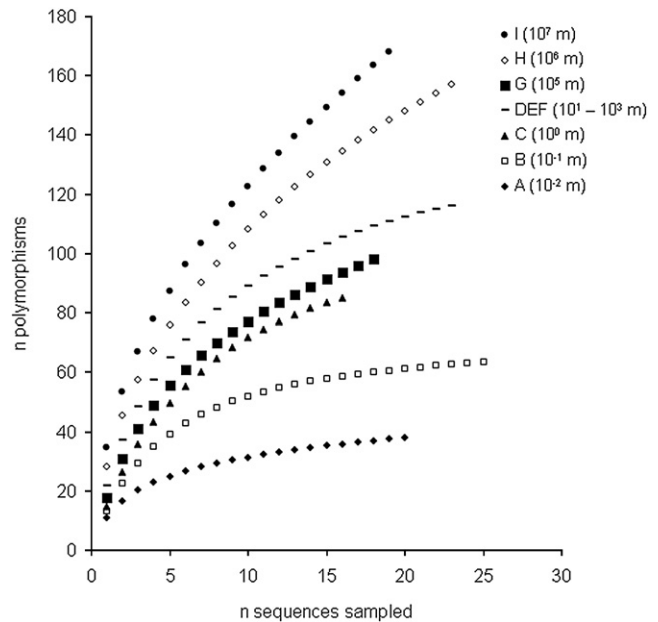


Figure 1. Rarefaction Curves of Sample Sets A–I

The number of polymorphisms in a five-locus, 2331 bp concatemer in each sample set is shown as a function of sub-sample size. Approximate within-sample-set distances are given in parentheses. All curves are significantly different from one another except C, D–F, and G, which do not differ from one another in any pairwise combination (see text).

were used in an analysis comparing diversity within (meter scale) versus between ( $10^5$ – $10^7$  m scale) transect populations. A total of ten such populations comprising 81 clones in total were utilized (Table S3).

Levels of genetic divergence across populations versus within populations were calculated with the  $F_{ST}$  index for all possible population pairs [22]. Most comparisons revealed significant genetic differentiation between populations ( $p < 0.05$  for 38 out of 45 pair-wise population comparisons). All of the exceptions are proximate populations within Europe, and the largest distance between nondifferentiated populations was 1680 km (Table S4). Not only were all more-distantly separated populations strongly differentiated from one another, but the degree of genetic differentiation between populations was found to correlate strongly with physical distance (Figure 3, Mantel  $r^2 = 0.36$ ,  $p < 0.001$ ).

Genetic divergence among population samples is consistently significant at distances greater than 2000 km and consistently insignificant at distances below 300 km (Figure 3). Together with the presence of a diversity plateau from the meter scale to the regional scale (Figures 1 and 2), these results indicate that the distribution of genetic diversity below a scale of  $\sim 10^5$  m is largely random and not limited by dispersal.

Why is diversity relatively even from the meter to regional scales but reduced below the meter scale (Figures 1 and 2)? This result could be due to the fact that not all common genotypes can be physically contained within areas below a certain threshold size. However, distinct *M. Xanthus* genotypes have been shown to co-occur at scales as small as centimeters [18]. The  $10^{-1}$  m scale at which diversity is reduced could therefore in theory contain as many concatemer genotypes as were found in southwest Germany.

Nucleotide diversity in the concatemer genes at the regional scale is likely to represent some degree of adaptive variation at

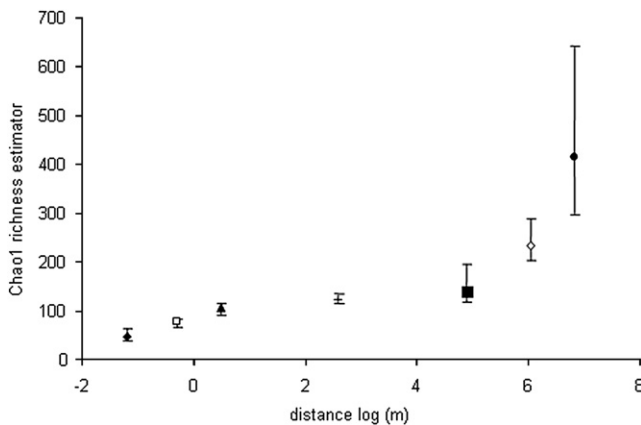


Figure 2. The Chao1 Total-Richness Estimator Plotted against Distance. Error bars indicate 95% confidence intervals. Symbol referents are the same as in Figure 1.

other loci in that at least some of the different genotypes are likely to have adapted to distinct niches within the soil. The fact that nucleotide variation in the concatemer genes remains similar from the meter scale to the regional scale (Figures 1 and 2) suggests that most *M. xanthus* niches present at the regional scale are also present at the meter scale. Diversity below the meter scale decreases steadily (Figures 1 and 2), suggesting that fewer niches are contained within successively smaller areas at our sample site. This scenario would suggest that most local adaptation to distinct niches within southwest Germany occurs in patches below the meter scale. Our data thus fit a model in which the same *M. xanthus* genotypes occur repeatedly throughout the region in small patches such that a similar degree of variation occurs across scales spanning  $10^1$ – $10^5$  m.

The substantial rise in diversity and population differentiation above the regional scale (Figures 1–3) might be caused by (1) genetic drift due to limited dispersal (i.e., isolation by distance), (2) the occurrence of a greater number of niches at greater scales (i.e., local adaptation), or (3) a combination of both. Given that the concatemer loci are selectively constrained, local adaptation at these five genes themselves is very unlikely. In theory, however, all five loci might have hitchhiked with loci that are indeed locally adapted, thus resulting in their increased diversity at greater scales. To circumvent this potentially complicating factor and more directly test whether dispersal is limited in *M. xanthus* at large scales, we analyzed patterns of diversity and population differentiation at a gene (*pilA*) that shows clear evidence of undergoing both adaptive diversification and recombination. These features promote the evolutionary independence of this locus relative to other loci.

The highly polymorphic *pilA* gene encodes the pilin subunit of type IV pili, which are necessary for social motility in *M. xanthus* [23] and several other functions in other bacterial species (e.g., [24–27]). A fragment of *pilA* was previously shown to be under diversifying selection in isolates sampled at the centimeter (A) scale via frequency distribution tests [18], a result further confirmed in this study by a per-codon  $d_N/d_S$  ratio test (Table S5). The selective forces underlying the diversification of *pilA* are unknown at present but might be related to the high degree of intra-specific social incompatibility observed in this species [28] (M.V. and G.J.V. unpublished data). Hitchhiking is unlikely to be of importance in *pilA* because (1) it is under

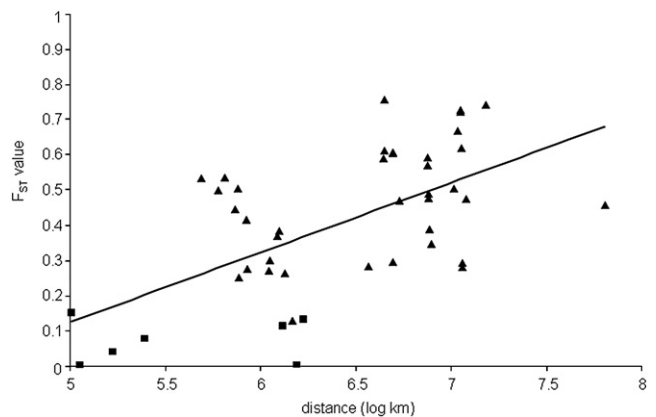


Figure 3.  $F_{ST}$  Values between Meter-Scale Populations Are Plotted against Inter-Population Distance

Significantly differentiated population pairs are indicated by triangles, and nonsignificantly differentiated population pairs are indicated by squares.  $F_{ST}$  values are based on a five-gene concatemer.

strong selection and (2) recombination in this locus is elevated in relation to the concatemer loci [18] (Table S6) and thus facilitates the evolutionary uncoupling of *pilA* from other genes.

As was observed for the multi-locus concatemer, *pilA* population divergence ( $F_{ST}$  Mantel  $r^2 = 0.23$ ,  $p < 0.001$ ), as well as nucleotide diversity ( $r^2 = 0.23$ ,  $p < 0.001$ ) increase significantly as a function of distance. Local adaptation might explain these patterns if increasingly larger areas house a greater range of distinct habitats that favor a greater range of functional variation in *pilA*. Alternatively, the increase in *pilA* diversity and differentiation with increasing scale might be due to limited dispersal and resulting genetic drift (i.e., isolation by distance). Under the isolation-by-distance hypothesis, functional variation present in *pilA* at small scales can be favored in a wide variety of habitats across large scales (global adaptation). The local-adaptation hypothesis implies that the rise in diversity of nonsynonymous (potentially adaptive) *pilA* variation with spatial scale should be steeper than that of synonymous (nonadaptive) variation. In contrast, the isolation-by-distance hypothesis implies that there should be no difference in the spatial patterns of diversity shown by nonsynonymous versus synonymous sites.

As predicted under the isolation-by-distance hypothesis,  $F_{ST}$  values calculated from synonymous *pilA* sites increase with distance to a degree similar to that of  $F_{ST}$  values calculated from nonsynonymous sites (Figure S4). Moreover, neither the strength of diversifying selection in *pilA* (as estimated by  $d_N/d_S$ ) nor the number of codons under selection was found to increase with spatial scale in the nested-isolate set (Figure S5). These spatial patterns of *pilA* variation are evidence that *M. xanthus* populations are isolated by distance.

Importantly, we note that the existence of isolation by distance at large scales ( $>10^5$  m) is fully compatible with the likely occurrence of local adaptation at other loci across variable environments. Given the wide variety of soils and climate zones from which *M. xanthus* can be isolated, there is great potential for local adaptation to be important at a wide range of scales [29]. Our concatemer and *pilA* data do not reveal the relative extent to which local adaptation and isolation by distance shape *M. xanthus* biogeography, but they do show that limited dispersal is a major determinant of spatial structure at large ( $>10^5$  m) scales.

The degree of population differentiation at *pilA* was found to be greatly reduced in relation to the concatemer loci (average  $F_{STpilA} = 0.20$  versus  $F_{STconc} = 0.41$ ,  $t = 5.05$ ,  $p < 0.0001$ ). This is expected for two reasons. First, because the within-population diversity of genes under diversifying selection is very high, between-population diversity is relatively low. Second, our results indicate that many *pilA* alleles can be favored in multiple habitats, possibly because negative frequency-dependent selection favors new alleles in a population regardless of their geographical origin. The effective migration rate of this gene may therefore be enhanced in relation to that of other genes, resulting in lower between-population diversity [30].

Our data suggest that high local diversity rather than enhanced allele spread is primarily responsible for the reduced  $F_{STpilA}$  values observed here (results not shown). Nonetheless, because *pilA* can be uncoupled from other loci by recombination (see above), *pilA* alleles might tend to migrate to a greater extent than the concatemer alleles. This scenario is suggested by five isolates from three continents that were found to share a single *pilA* allele despite having diverged substantially at several concatemer loci (Table S7).

In his 1934 treatise on microbial biogeography, Baas Becking postulated that “everything is everywhere, but the environment selects” [31]. In his view, the ubiquity and small size of microbes would result in unlimited dispersal, but the omnipresence of any particular type of microbe would only be revealed under environmental conditions that allow growth. In contrast, this study demonstrates that limited dispersal can generate population structure even in a broadly distributed, spore-forming soil bacterium. The results presented here also highlight the importance of taking population structure and gene function into account when estimating microbial diversity.

## Experimental Procedures

### Isolate Collection

A nested-sampling design was employed with soil samples collected at nine different spatial scales (Table 1). Isolates were assigned to one scale only, making the different sets completely independent. The first four scales were nested-sampling grids centered in a woodlot in Tübingen, Germany: set A was at the centimeter scale, set B was at the decimeter scale, set C was at the meter scale, and set D had samples scattered across an ~100 m × 100 m grid. The next scales consisted of two 10<sup>2</sup> and 10<sup>3</sup> m transects (sets E and F, respectively) and samples collected at different locations in southwestern Germany (set G), across Europe (set H), and across the globe (outside Europe) (set I). We refer to this set of nested samples as the nested-isolate (or sample) set (Table 1).

The pair-wise spatial distances between isolates within a given set were mostly smaller or greater within the next larger or smaller scale sets, respectively, and there were very few instances of distance overlap between sets. The distances between isolation points ranged from 1.7 to 13.7 cm for sample set A (10<sup>-2</sup> m scale), 10 to 141 cm for set B (10<sup>-1</sup> m scale), 1.0 to 7.2 m for set C (10<sup>0</sup> m scale), 10 to 83 m for set D (10<sup>1</sup> m scale), 88 to 788 m for set E (10<sup>2</sup> m scale), 200 to 1800 m for set F (10<sup>3</sup> m scale), 4 to 239 km for set G (10<sup>5</sup> m scale), 66 to 3278 km for set H (10<sup>6</sup> m scale), and 433 to 17,536 km for set I (10<sup>7</sup> m scale).

At most sampling locales for sets G, H, and I, ten soil samples were collected at 1 m intervals in a linear transect. When multiple *M. xanthus* clones could be isolated from a transect, the first isolate in the transect was added to the nested-isolate set. When isolates could be obtained from six or more sample points within a single transect, they were used for comparing diversity within transect populations to diversity between transect populations. We refer to this set of isolates as the population isolate set (Table S3).

For a detailed description of the isolation of single clones, see reference [18]. In short, soil samples were dispersed on selective medium that did not contain compounds that target Gram-negative bacteria, and therefore no selective bias in the isolation of particular *M. xanthus* strains was imposed. Fruiting bodies were picked from soil particles with sterile toothpicks. Samples were incubated at 50°C for 2 hr and sonicated twice for 10 s

with a tip sonicator so that non-spores would be killed and spores would be dispersed. Spore suspensions were diluted into melted CTT soft agar (50°C) supplemented with antibiotics. After about 5 days, one colony (derived from a single spore) was randomly picked and transferred to a new selective plate. Finally, clones were grown in liquid medium for DNA isolation and frozen storage (-80°C in 20% glycerol). Genomic DNA was isolated with an MBI Fermentas Genomic DNA Purification Kit.

The 16S rRNA gene was sequenced in 49 isolates from the population dataset and nested-isolate sets H and I and was compared to reference strain DK1622 so that species identification could be confirmed. No nucleotide polymorphisms were found in the 650 bp alignment. Table S1 lists all isolates, locations, coordinates and soil samplers. Soil samplers were provided with a common sampling protocol and asked to sample from any location that was pristine or had apparently been undisturbed for a long period, regardless of habitat.

### PCR Amplification and DNA Sequencing

Segments of five loci were initially sequenced in all isolates: the ATP-dependent Clp protease ATP-binding subunit *clpX*, the developmental C-signal *csgA*, a putative zinc metalloprotease associated with the extra-cellular fibril-matrix *fibA*, isocitrate dehydrogenase *icd*, and *dnaK* homolog (HSP70 chaperone) *sglK*. Multi-locus sequence-typing (MLST) studies typically make use of selectively constrained loci. *clpX*, *icd*, and *sglK* loci are commonly used for MLST purposes; the *fibA* and *csgA* loci in *M. xanthus* were previously shown to be selectively constrained and so are suitable as well [18]. Primer sequences are listed in the Tables S8 and S9. The quality of sequence trace files was evaluated by eye with Seqman II software (DNASTAR, Madison, WI). Sequences were aligned with the CLUSTAL W algorithm implemented in MEGA version 3.0 [27, 32] ([www.megasoftware.net](http://www.megasoftware.net)). To allow for a direct comparison between populations, the alignments of each locus were cut to maximum shared length. The five loci were analyzed both separately and as a concatemer sequence. A unique combination of five alleles is considered here to be a unique genotype (or “sequence type”). In addition, a fragment of the pilin (type IV pilus subunit)-encoding gene *pilA* was sequenced for all isolates. Because these sequences were highly variable, they were translated for alignment with the CLUSTAL W algorithm and then untranslated for DNA analysis.

### Rarefaction Curves

A concatemer alignment of all isolates was generated with variable sites only. The presence or absence of nucleotide polymorphisms in every sequence was scored so that a nucleotide-incidence matrix could be created. Every polymorphism rather than every polymorphic site was scored because an appreciable number of sites segregated for three nucleotides (i.e., three different nucleotides were found at the same site across genotypes). These scores were used as input for the program EstimateS 7.5 [28, 33] (<http://viceroy.eeb.uconn.edu/EstimateS>). To our knowledge, this is the first time the rarefaction method has been applied to individual nucleotide polymorphisms.

We treated individual sequences as samples and individual polymorphisms as ‘species’ (sample-based rarefaction) rather than treat nucleotide sites as individuals and polymorphisms as a species (individual-based rarefaction). This is because polymorphisms are likely to be in linkage disequilibrium at the scale of individual loci (i.e., they are associated with each other due to largely clonal reproduction). To clarify the differences between the sample- and individual-based approach Gotelli and Colwell [29] give the following example. A survey of plant diversity will be higher when plants in a plot are randomly sampled (individual-based assessment) than if a number of quadrats in a plot are sampled (sample-based assessment) due to the spatial clustering of individuals belonging to the same species. A sample-based rarefaction curve therefore generally lies below an individual-based rarefaction curve [29]. We used a computationally fast analytical method [19] with results indistinguishable from the classic random sub-sampling method implemented in the program EstimateS 7.5 [28, 33] to create sample-based rarefaction curves. (Note: A programming error in the Chao variance estimators has been corrected in EstimateS version 8.0 subsequent to our data analysis. A re-run of a subset of our data in version 8.0 did not change the results, revealing that our initial data analysis was not affected by this programming error).

EstimateS 7.5 was also used for calculating the Chao1 richness estimator along with log-linear 95% confidence intervals [30]. Chao1 was calculated with classic or bias-corrected equations depending on the recommendation prompted by EstimateS for the sample set in question. We used the maximum sample size in each set to calculate Chao1 so that we could obtain

the best possible estimate per set (Figure 2). However, the differences in Chao1 between different sets remain qualitatively similar when sampling sets are compared at maximum shared sample size.

#### Genetic Divergence between Populations

Pairwise  $F_{ST}$  values were calculated for ten populations collected across the world (Table S4). The  $F_{ST}$  index is defined as the ratio of between-population diversity ( $\pi_S$ ) relative to total diversity ( $\pi_T$ ) ( $(\pi_T - \pi_S)/\pi_T$ ). Pairwise  $F_{ST}$  values range between 0 and 1; values above 0.15 are usually taken to indicate great genetic differentiation [31]. Analyses were performed on the concatemer sequence with the program DnaSP 4.0. We obtained the null distribution of  $F_{ST}$  values by randomly assigning isolates to populations (1000 replicates). The  $p$  value of the test refers to the proportion of randomizations with an equal or higher-than-observed  $F_{ST}$  value. The Mantel regression coefficient for the pairwise  $F_{ST}$  values was calculated with the program zt [34] (available at <http://www.psb.ugent.be/~erbon/mantel/>).

#### Spatial Analysis

Distances between sampling points were measured on site for the small-scale sets (A, B, C, D, and within-transsect samples for isolate set Y) and measured on a map for the intermediate-scale sets (E and F). For sets G, H, and I, coordinates of sampling locations were, if not supplied by the soil sampler, retrieved with Google Earth (<http://earth.google.com>). The distance between different sampling locations was then calculated with the ARC\_CALC\_3 Spherical Trigonometry Calculator macro (available at: [http://www.jqjacobs.net/astro/arc\\_form.html](http://www.jqjacobs.net/astro/arc_form.html)) written for Excel by James Q. Jacobs.

#### Accession Numbers

All nucleotide sequences analyzed in this study have been deposited in GenBank. The sequences in sample set A have been analyzed previously; their accession numbers can be found in [18]. Accession numbers of sequences in sample sets B–G are as follows: *icd*, EF111265–EF111446; *sglK*, EF111447–EF111628; *clpX*, EF111629–EF111810; *csgA*, EF111811–EF111992; *fibA*, EF111993–EF112174; and *pilA*, EF526567–EF526586.

#### Supplemental Data

Nine supplemental tables and five supplemental figures are available online at <http://www.current-biology.com/cgi/content/full/18/5/386/DC1/>.

#### Acknowledgments

We thank Heike Keller for sequencing, Tamara Riedt and Jochen Reiter for help with isolation, Daniel Wilson and Gil McVean for advice on omegaMap, and Nick Barton, Thomas Bell, Angus Buckling, Fred Cohan, Matt Hahn, John Pannell, and Christopher van der Gast for helpful suggestions and/or comments on the manuscript. We thank all who contributed soil samples to this project. This work was supported by the Max-Planck Society and a grant from the Deutsche Forschungsgemeinschaft (DFG VE 362/1-2).

Received: November 9, 2007

Revised: January 14, 2008

Accepted: February 5, 2008

Published online: March 6, 2008

#### References

- Green, J., and Bohannan, B.J. (2006). Spatial scaling of microbial biodiversity. *Trends Ecol. Evol.* 21, 501–507.
- Martiny, J.B., Bohannan, B.J., Brown, J.H., Colwell, R.K., Fuhrman, J.A., Green, J.L., Horner-Devine, M.C., Kane, M., Krumsins, J.A., Kuske, C.R., et al. (2006). Microbial biogeography: Putting microorganisms on the map. *Nat. Rev. Microbiol.* 4, 102–112.
- Papke, R.T., Ramsing, N.B., Bateson, M.M., and Ward, D.M. (2003). Geographical isolation in hot spring cyanobacteria. *Environ. Microbiol.* 5, 650–659.
- Papke, R.T., and Ward, D.M. (2004). The importance of physical isolation to microbial diversification. *FEMS Microbiol. Ecol.* 48, 293–303.
- Whitaker, R.J. (2006). Allopatric origins of microbial species. *Philos. Trans. R. Soc. Lond. B Biol. Sci.* 361, 1975–1984.
- Fenchel, T. (2003). Microbiology. Biogeography for bacteria. *Science* 301, 925–926.
- Escobar-Paramo, P., Ghosh, S., and DiRuggiero, J. (2005). Evidence for genetic drift in the diversification of a geographically isolated population of the hyperthermophilic archaeon *Pyrococcus*. *Mol. Biol. Evol.* 22, 2297–2303.
- Whitaker, R.J., Grogan, D.W., and Taylor, J.W. (2003). Geographic barriers isolate endemic populations of hyperthermophilic archaea. *Science* 301, 976–978.
- Buckley, D.H., Huangyuthitam, V., Nelson, T.A., Rumberger, A., and Thies, J.E. (2006). Diversity of Planctomycetes in soil in relation to soil history and environmental heterogeneity. *Appl. Environ. Microbiol.* 72, 4522–4531.
- Cho, J.C., and Tiedje, J.M. (2000). Biogeography and degree of endemicity of fluorescent *Pseudomonas* strains in soil. *Appl. Environ. Microbiol.* 66, 5448–5456.
- Fulthorpe, R.R., Rhodes, A.N., and Tiedje, J.M. (1998). High levels of endemicity of 3-chlorobenzoate-degrading soil bacteria. *Appl. Environ. Microbiol.* 64, 1620–1627.
- Glaeser, J., and Overmann, J. (2004). Biogeography, evolution, and diversity of epibionts in phototrophic consortia. *Appl. Environ. Microbiol.* 70, 4821–4830.
- Neilan, B.A., Saker, M.L., Fastner, J., Torokne, A., and Burns, B.P. (2003). Phylogeography of the invasive cyanobacterium *Cylindrospermopsis raciborskii*. *Mol. Ecol.* 12, 133–140.
- Ramette, A., and Tiedje, J.M. (2007). Multiscale responses of microbial life to spatial distance and environmental heterogeneity in a patchy ecosystem. *Proc. Natl. Acad. Sci. USA* 104, 2761–2766.
- Sikorski, J., and Nevo, E. (2005). Adaptation and incipient sympatric speciation of *Bacillus simplex* under microclimatic contrast at “Evolution Canyons” I and II, Israel. *Proc. Natl. Acad. Sci. USA* 102, 15924–15929.
- Silva, C., Vinuesa, P., Eguiarte, L.E., Souza, V., and Martinez-Romero, E. (2005). Evolutionary genetics and biogeographic structure of *Rhizobium gallicum sensu lato*, a widely distributed bacterial symbiont of diverse legumes. *Mol. Ecol.* 14, 4033–4050.
- Dawid, W. (2000). Biology and global distribution of myxobacteria in soils. *FEMS Microbiol. Rev.* 24, 403–427.
- Vos, M., and Velicer, G.J. (2006). Genetic population structure of the soil bacterium *Myxococcus xanthus* at the Centimeter Scale. *Appl. Environ. Microbiol.* 72, 3615–3625.
- Colwell, R.K., Mao, C.X., and Chang, J. (2004). Interpolating, extrapolating, and comparing incidence-based species accumulation curves. *Ecology* 85, 2717–2727.
- Hughes, J.B., Hellmann, J.J., Ricketts, T.H., and Bohannan, B.J.M. (2001). Counting the uncountable: statistical approaches to estimating microbial diversity. *Appl. Environ. Microbiol.* 67, 4399–4406.
- Roberts, M.S., and Cohan, F.M. (1995). Recombination and migration rates in natural populations of *Bacillus subtilis* and *Bacillus mojavensis*. *Evolution Int. J. Org. Evolution* 49, 1081–1094.
- Wright, S. (1951). The genetic structure of populations. *Ann. Eugen.* 15, 323–354.
- Wu, S.S., and Kaiser, D. (1995). Genetic and functional evidence that type IV pili are required for social gliding motility in *Myxococcus xanthus*. *Mol. Microbiol.* 18, 547–558.
- Graupner, S., Frey, V., Hashemi, R., Lorenz, M.G., Brandes, G., and Wackernagel, W. (2000). Type IV pilus genes *pilA* and *pilC* of *Pseudomonas stutzeri* are required for natural genetic transformation, and *pilA* can be replaced by corresponding genes from nontransformable species. *J. Bacteriol.* 182, 2184–2190.
- van Schaik, E.J., Giltner, C.L., Audette, G.F., Keizer, D.W., Bautista, D.L., Slupsky, C.M., Sykes, B.D., and Irvin, R.T. (2005). DNA binding: A novel function of *Pseudomonas aeruginosa* type IV pili. *J. Bacteriol.* 187, 1455–1464.
- Craig, L., Pique, M.E., and Tainer, J.A. (2004). Type IV pilus structure and bacterial pathogenicity. *Nat. Rev. Microbiol.* 2, 363–378.
- Kim, T.J., Lafferty, M.J., Sandoe, C.M., and Taylor, R.K. (2000). Delineation of pilin domains required for bacterial association into microcolonies and intestinal colonization by *Vibrio cholerae*. *Mol. Microbiol.* 35, 896–910.
- Fiegna, F., and Velicer, G.J. (2005). Exploitative and hierarchical antagonism in a cooperative bacterium. *PLoS Biol.* 3, e370.
- Belotte, D., Curien, J.B., Maclean, R.C., and Bell, G. (2003). An experimental test of local adaptation in soil bacteria. *Evolution Int. J. Org. Evolution* 57, 27–36.

30. Schierup, M.H., Vekemans, X., and Charlesworth, D. (2000). The effect of subdivision on variation at multi-allelic loci under balancing selection. *Genet. Res.* 76, 51–62.
31. Baas Becking, L.G.M. (1934). *Geobiologie of inleiding tot de milieukunde* (Den Haag, The Netherlands: WP Van Stockum & Zoon NV).
32. Kumar, S., Tamura, K., and Nei, M. (2004). MEGA3: Integrated software for molecular evolutionary genetics analysis and sequence alignment. *Brief. Bioinform.* 5, 150–163.
33. Colwell, R.K. (2005). EstimateS: Statistical estimation of species richness and shared species from samples. *Version 7.5*. <http://purl.oclc.org/estimates>.
34. Bonnet, E., and Van de Peer, Y. (2002). zt: A software tool for simple and partial Mantel tests. *Journal of Statistical Software* 7.